IJBEM
Vol. 7, No. 1, 2005

Simulated Comparison of Disc and Concentric Electrode Maps During Atrial Arrhythmias.

Venkatesh Soundararajan [1],W. G. Besio [1]
[1]Department of Biomedical Engineering, Louisiana Tech University, Ruston, LA, USA

Abstract— **Cardiac electrical activity, which drives the rhythmic pumping action of the heart, is spatio-temporal in nature. 12-Lead ECG, the conventional non-invasive technique used to diagnose heart diseases, provides good temporal information and by adding more electrodes body surface potential maps (BSPM) have been used to improve spatial resolution. Recently mapping of body surface Laplacian (BSLM), which is the second derivative of potential, was used to enhance spatial resolution further.**

There has been no computer model development reported to create BSPM and BSLM using bi and tri-polar concentric ring Laplacian electrodes. The authors report on computer model of human heart and torso with an array of concentric ring electrodes over the surface of the torso. Conduction of action potentials through the heart under normal conditions and certain atrial arrhythmias were modeled and BSPMs and BSLMs were created. It was found that tripolar concentric electrodes provide better spatial resolution than bipolar concentric electrodes and could be used to detect atria related arrhythmias.

Keywords— **Atrial arrhythmias, Body surface potential map, BSPM, Body surface Laplacian map, BSLM, Bipolar electrode, concentric rings, ECG, localization capability, Tripolar electrode.**

I. INTRODUCTION

12-Lead electrocardiogram (ECG) has been the conventionally used non-invasive technique for diagnosing cardiac diseases. It provides good temporal information regarding cardiac activity. To obtain better spatial information of underlying cardiac activity, more recording leads covering a greater body surface have been used to create BSPM [1]. Spatial content of BSPMs due to cardiac electrical activity have been limited by the smearing effect of the torso volume conductor. To over come the smoothing effect of the torso volume conductor, mapping of Laplacian potentials, the second derivative of surface potentials, was proposed and found to provide better spatial localization of multiple cardiac events [2].

In 1975, Hjorth [2], first used surface Laplacian for recording EEG. He [1] developed a non-invasive approach to directly measure body surface Laplacian potentials using dry bipolar Laplacian electrodes. It was found that BSPM could resolve multiple sources only when they were separated by a distance greater than the distance of the source to electrode [1]. BSLM showed superior ability to distinguish multiple sources [1-2,6-8].

Wu [7] used a finite element heart model to conduct a computer simulation study to investigate the performance of BSLMs. A two site pacing protocol was used for the simulation and instantaneous BSPMs and BSLMs (using analytical Laplacian potentials), with varying distances between the pacing sites. In order to quantify the capability of body surface maps in separating two myocardial electrical events, a parameter called the separation coefficient (SC) [7] was introduced. The SC's of BSLMs and BSPMs for various distances between pacing sites were compared and it was shown that BSLM can better localize and image multiple simultaneously active myocardial electrical events.

Besio [4-6] developed a Laplacian electrocardiogram (LECG) system to study cardiac activation patterns including those of the atria, which are much weaker than those of ventricles. They used quasi-bipolar electrodes, which are tripolar electrodes with the center disc shorted to the outer ring, for their recordings on healthy and atrial flutter subjects. It was demonstrated that an active LECG sensor system could better aid in detection of atrial activity.

Recently, Besio [12], in 2004, reported developing a tripolar electrode configuration based on a nine-point finite difference method. A computer simulation and tank experiment was carried out to compare the localization capabilities of bipolar, quasi-bipolar and tripolar electrode configurations. It was found that the localization capability of the tripolar electrode configuration was significantly better than that of the other configurations.

No literature has been found reporting modeling tripolar concentric ring electrodes on the body surface other than from Besio [7]. To continue the exploration of tripolar Laplacian electrodes, a computer model was developed that would compare the spatial localization capabilities of bipolar and tripolar Laplacian electrodes for detection of atrial arrhythmias. The complexity of this model will continue to evolve with future work.

II. METHODOLOGY

A human heart-torso and concentric ring electrode model was developed using MATLAB (Version 6.Release 13, Math works). The human heart was modeled as a sphere, as shown in Fig.1.a, of radius 5 cm, consisting of 20 cross-sections along planes perpendicular to the base to apex axis. The distance between adjacent sections was 2.5mm. The upper hemisphere represented the atria, the lower hemisphere represented the ventricles and the line passing through the center of the lower hemisphere

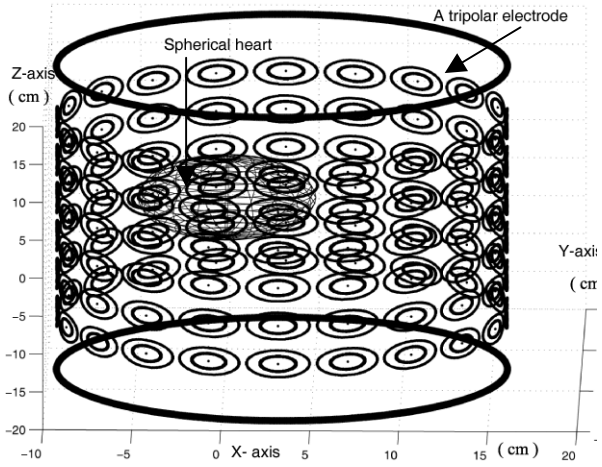

Fig. 1: The heart-torso model wrapped with a 6x18 array of concentric ring sensors.

represented the bundle of His. The number of slices of the heart is variable to adjust the resolution.

The human torso, truncated at the neck, waist and arms, was modeled as a cylinder of circumference 100 cm and a height of 40 cm as shown in Fig.1. The cylindrical surface of the torso was divided into 2000 vertical slices. Each vertical slice was further divided into 0.5 mm high horizontal slices. Thus the entire surface of the cylinder was represented by a grid of resolution 0.5 mm. This resolution could be set to any desired value by changing the number of vertical and horizontal slices on the torso. Of course there are practical limits, such as the time it takes to complete all the calculations. The resolution determined the density of points that constituted the center disc, inner and outer ring of each electrode.

The surface potential at every point on the torso model due to a charge q**,** located in the heart, is given by

$$v = qz/4\pi\varepsilon_r\varepsilon_0\, r^{3/2} \qquad (1)$$

where ε_0 is the permittivity of free space, ε_r is the relative permittivity, **z** is the distance between the dipole and center of the disc, and **r** is the distance between the dipole and point of measurement (points on the disc or any of the two rings of the electrode). The average of potentials measured, using (1), at all the points constituting the elements of each electrode would give the potentials on the disc, middle and outer rings of each electrode.

In the computer model of the tri-polar concentric ring electrode array that we developed, the radius of the center disc was 2 mm, the inner ring was 1.2 mm thick with an inner radius of 0.94 cm and outer ring was 0.5 mm thick with an inner radius of 1.75 cm. A 6x18 array of concentric ring electrodes was developed to encompass the cylindrical torso, as shown in Fig.1. However the entire back of the torso was not covered with electrodes. This was to provide for translation of the electrode array, which is explained later.

Hjorth [2] recorded the Laplacian of surface potentials using a finite difference five-point method (FPM). Two methods, namely five point and nine point finite difference methods for calculation of body surface Laplacian potentials have been implemented in the model reported now. Potentials at 6 x 18 points on the surface of a cylindrical torso were calculated at each instant of the depolarization wave through the heart. The entire grid of 6 x 18 points of interest was translated 9 times in 5mm increments and potentials calculated at each position. BSPMs and BSLMs were generated with appropriate boundary conditions. For the purpose of surface potential calculations, the heart model was divided into 20 slices and the resultant dipole for each slice was assumed to act at the center of that slice [10]. Thus for one depolarization cycle the action potential moved through 10 atrial slices, then 10 His cells and finally through 10 ventricular slices.

To determine the magnitude of dipoles for each slice, the values of q, ε_r, ε_0 in the factor $q/4\pi\varepsilon_r\varepsilon_0$ in (1) were adjusted through trial and error process until lead-II potential tracings over one normal cardiac depolarization cycle resembled a real Lead-II ECG recording [10]. The values of this factor obtained through this trial and error process are assumed to represent the charge at each slice of the heart and are used in further calculation of potentials during creation of body surface potential/Laplacian maps.

A finite difference nine-point method (NPM) to approximate the Laplacian of potential has been reported [9,12]. Based on the NPM, a tripolar electrode was developed and an approximation to the Laplacian potential measured by

$$V_{Laplacian} = [16(Vm - V_c) - (V_o - V_c)] \qquad (2)$$

where V_m, V_o and V_c are the potentials on the middle ring, outer ring and the center disc of the electrode.

Implementation of the FPM results in an approximation of a bipolar electrode configuration with the middle ring of the tripolar configuration removed. The Laplacian potentials are calculated by the formula;

$$V_{Laplacian} = [(V_o - V_c)] \qquad (3)$$

In order to quantify the capability of body surface maps in separating two cardiac electrical events the SC introduced by Wu [7] was used. The separation coefficient was given as

$$sc = (a1 + a2)/(b1 + b2) \qquad (4)$$

where the terms a1, a2, b1, and b2 are marked in Fig.2. Sharper peaks would have greater separation coefficient.

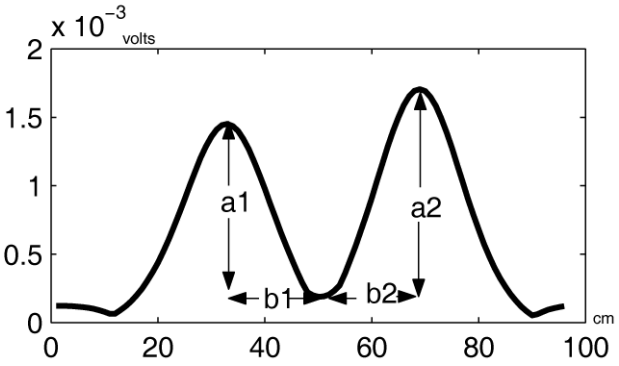

Fig. 2: Illustration of separation coefficient variables

III. RESULTS

In Fig.3 through Fig.5, subplot-A shows a BSPM, subplot-B BSLM calculated by the FPM, subplot-C the BSLM using the NPM and subplot-D Lead-II depolarization potentials calculated by the model. In Fig.3 Each panel was calculated at His cell number eight during conditions of normal action potential propagation. In each of the subplots, the part to the left of the second vertical line from left represents the chest and that on right represents the back of the torso. The white vertical line is the midsternal line and the horizontal line is the line passing through the nipples

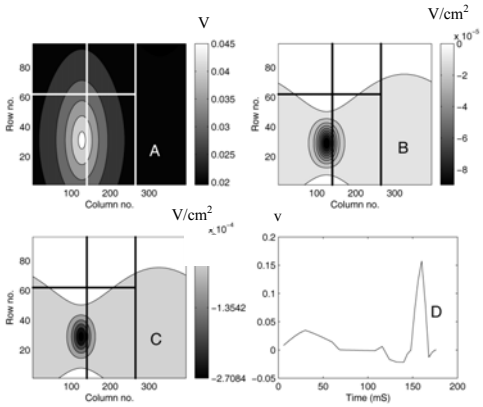

Fig.3 A) BSPM B) BSLM by FPM C) BSLM by NPM all under normal conditions.

In all the BSPM/BSLM plots, the X-axis represents column numbers and the Y-axis row numbers on the surface of the torso. The distance between any two columns/rows was 5 cm, which is the distance by which the electrode array was incrementally translated.

In Fig.4, each panel was calculated under conditions of PSVT. It can be seen in subplot 4-D that the P-wave is inverted due to retrograde propagation of action potential through the atria, which happens in the case of PSVT. The maps for PSVT are generated when the action potentials are at atrial slice number three and His cell number eight. In subplots 4-B, 4-C, 5-B, and 5-C two sets of concentric areas, termed "(a)" and "(b)", are evident. The set "(a)" indicates presence of an atrial source and the set "(b)" indicates presence of a ventricular source.

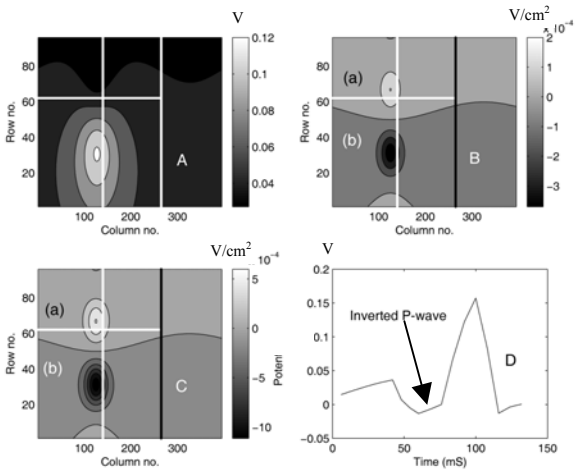

Fig.4 A) BSPM B) BSLM by FPMC) BSLM by NPM all under conditions of PSVT

In Fig.5, each panel was calculated under conditions of atrial flutter. PSVT The two P-waves in subplot 5-D, marked "a" and "b", are due to the 2:1 conduction block that was simulated for atrial flutter. The P-wave "a" resulted in a corresponding QRS complex and the P-wave "b" was blocked at the AV node. The maps for PSVT are generated when the action potentials are at atrial slice number and His cell number seven

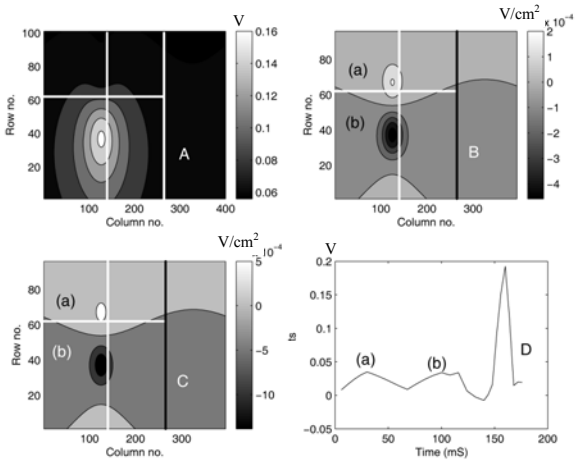

Fig.5 A) BSPM B) BSLM by FPM C) BSLM by NPM all under conditions of atrial flutter.

Fig.6 shows the BSP and Laplacian potential by the FPM and NPM at an instant when the sources are at atrial slice number five and His cell number ten, similar to a condition that occurs during PSVT.

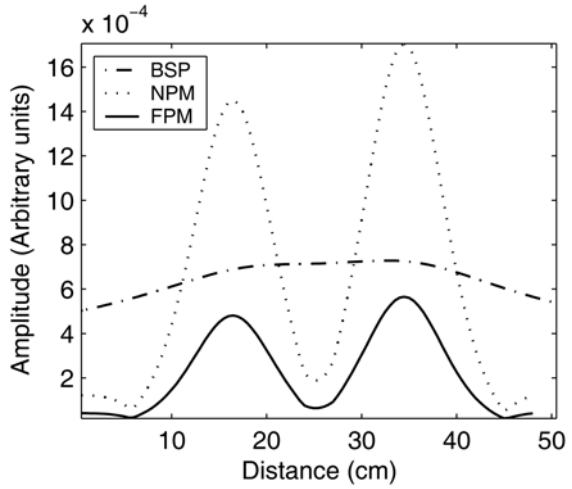

Fig 6: BSP, Laplacian potential by FPM and NPM during PSVT.

Table1 provides the SC values of BSP, Laplacian potentials by FPM and NPM for the aforesaid instant of PSVT.

Table I: Separation coefficients

Body surface potential	1.2458e-005
Body surface Laplacian potential using FPM	2.3137e-005
Body surface Laplacian potential using NPM	7.0017e-005

IV. DISCUSSION

In the present computer simulation study, we have investigated the performance of the BSLMs to spatially localize multiple cardiac electrical events that occur during conditions of atrial arrhythmias. This characteristic of BSLMs might be useful in detecting and spatially localizing multiple cardiac sources. The results of the computer simulations confirm previous experimental and simulation findings [1,7-8] that BSLMs provide better spatial localization compared to BSPMs.

The FPM is an approximation to a "disc and ring" bipolar electrode configuration where the average of the potentials from the outer points form what would be measured by the ring. The NPM uses four more distant points from the center to approximate potential that would be measured by a third element of a tripolar ring electrode configuration. It was proven that for a bipolar electrode configuration, sources not at the center of the electrodes are attenuated by $1/r^4$ [11]. By adding the extra ring, the attenuation of distant sources is further enhanced and this is why the tripolar electrode configuration results in an improved SC over the bipolar electrode configuration, Table I

V. CONCLUSION

The NPM has the highest SC and hence offers better spatial resolution than BSPMs from disc electrodes and BSLMs from the FPM.

With this we can conclude that body surface Laplacian mapping based on the NPM might be used to detect atrial arrhythmias, wherein atrial activity happens in the presence of ventricular depolarization.

REFERENCES

[1] B.He and R.J.Cohen, " Body surface Laplacian ECG mapping", IEEE transactions on BME, vol.39, No.II, November1992

[2] B.Hjorth, "An online transformation of EEG scalp potentials into orthogonal source derivations", EEG and clin. Neurophysiology, vol.39, pp.526-530, 1975.

[3]] W.Besio, C.Lu and P.Tarjan, "A feasibility study for body surface cardiac propagation maps of humans from Laplacian moments of activation" Electromagnetics, vol. 21, pp. 621-632, 2001.

[4] W. Besio, and P. Tarjan, "Arial activation pattern from surface Laplacian electrocardiograms of humans," International Journal of Bioelectromagnetism, vol.4, pp. 95-96, 2002.

[5] W.Besio and P.Tarjan, "Filtering of surface Laplacian electrocardiograms from humans to produce atrial activation patterns," *Proc. of 24th Annual International Conference of the IEEE EMBS and the 2002 Fall Meeting of the BMES pp.255*

[6] W.Besio, K.Koka, and R.Patwardhan, "Computer simulation and tank experimental verification of concentric ring electrodes", *Proc. of 24th Annual International Conference of the IEEE EMBS, Sept 2004, pp.2243.*

[7] D.Wu, K.Ono, H.Hosaka and B.He, "A simulation study of body surface Laplacian maps during ventricular pacing in a 3D inhomogeneous heart-torso model", *Proc. of BSI99.*

[8] B.He, A.Tsai and R.J.Cohen, "A simulation study of body surface Laplacian ECG maps using a spherical volume conductor model"

[9] R.Aakula, "Theoretical background and design of tri-polar concentric ring sensor", Masters Thesis, Louisiana Tech University, 2004

[10] M.Lorange and R.M.Gulrajani, "A computer heart model incorporating anisotropic propagation", Journal of electrocardiology vol.26 No.4 1993.

[11] J.Strackee and A.Van Oosterom, "Computing the lead field of electrodes with axial symmetry", Medical and biological engineering and computing, , vol21, pp.473-481, 1993

[12] W.Besio, R.Akula and W.Dai, "Comparison of bipolar and tripolar concentric electrode Laplacian estimates", *Proc. of 26th Annual International Conference IEEE EMBS, pp.2255-2258, 2005*